Surface Reaction Characteristics and Oxygen Evolution Capability of a Pd80at.%Ni Electrode in 30wt.%KOH medium

R. Das[1], M. Shajahan[1], A. K. M. A. Ullah[2], H. M. B. Alam[3] and A. K. M. F. Kibria[3*]

[1]*Department of Chemistry, Jagannath University, Dhaka, Bangladesh*
[2]*Chemistry Division, Atomic Energy Centre, Dhaka, Bangladesh*
[3,*]*Nuclear Safety, Security and Safeguards Division, Bangladesh Atomic Energy Commission, Dhaka, Bangladesh*

Abstract

In view to finding an efficient electrode for oxygen evolution through water electrolysis, the surface reaction characteristics and the oxygen evolution efficiency of a Pd80at.%Ni electrode was investigated in 30wt.%KOH electrolyte at 298 K using Cyclic Voltammetry (CV). The CV diagrams of the electrode showed two oxidation and two reduction peaks while cycling in between the potential range of – 1.0 to + 0.65 V at different scan rates. A time dependent study enabled to obtain the saturated layer of (PdNi)(III) species over the electrode surface after 100 minutes of cycling. This species realized to be crucial for the generation of atomic oxygen and thereafter for oxygen evolution. Tafel plot for the oxygen evolution reaction (OER) showed two well-defined Tafel regions. Kinetic parameters, i.e., the exchange current density at zero overpotential (i_0) and the slope (b) values for the low and high overpotential (η) regions were found to be 2.83 x 10^{-3} and 2.35 mA/cm^2 and 72.8 and 215.1 mV/dec, respectively. Observed i_o value for the low η region is equal to that of Ni electrode but that of the high η region is more than 21 times higher than that of Ni electrode. Thus, Pd80at.%Ni electrode can be considered to be an efficient electrode for the production of oxygen through electrolysis.

Keywords: Pd80at.%Ni electrode, oxygen evolution, oxidation-reduction, Tafel plot, kinetic parameters, exchange current density

1. Introduction

Oxygen evolution reaction (OER) is an important half-cell reaction which appears in an electrolyzer during the electrolysis of water. Research on this attractive and important reaction has been intensely carried out for decades [1-5]. In practices, OER is such a reaction step that must compose of four electron transfers and oxygen-oxygen bond formation [6, 7]. Such a reaction usually is not favored kinetically and thereby requires catalyst for expediting it. Usually OER involves multiple electrochemical steps with at least one electron transfer per step [8, 9]. As it is an electron-coupled uphill reaction, input of electricity is needed as energy to drive the water splitting reaction. The standard potential for OER is 1.23 V *vs* Reversible hydrogen electrode (RHE). An accumulation of energy barrier in each reaction step leads to a sluggish kinetics of OER to overcome this large potential. Therefore, the OER electrocatalysis is desired to expedite the reaction and lower the potential. As very few non-precious metal oxides can survive under oxidative potential in acidic condition [10], researchers have been searching for non-precious metal-based hetero catalysts for the OER electrocatalysis in alkaline conditions in which surface metal oxides or hydroxides are chemically stable. An ideal OER electrocatalyst should have low overpotential, high durability, low-cost and economical and earth-abundance. However, catalysts meeting such requirements have not yet been found. Therefore, the selection of OER electrode material(s) is not at all an easy task. The best performing electrode such as Pt, Pd, Ru are highly expensive, while the cheaper substituents using less noble metals suffer from corrosion, passivation or both the problems [11].

*Corresponding author: e-mail: kibriaf@yahoo.com

Now-a-days, reports are available that Ni and Ni-based materials can play a key role as oxygen evolution catalysts in alkaline electrolysis [3, 12]. Until today, Ni-based oxides are widely used since they show good activity and have high resistance to corrosion in the alkaline media [13, 14]. It is well established that potential cycling can cause transformations between the forming phases of hydroxides and oxides in nickel and nickel-based electrodes with different oxidation states and crystallinities [3, 14]. Upon continuous cycling in a chosen range of potential, the top hydrous nickel oxide film grows progressively, which is responsible for enhancing activity toward the OER [3, 15].

The elctrocatalytic behavior and the hydrogen evolution efficiency of Pd [16] and Ni [3, 17] electrocatalysts are well documented. It has been observed that Pd based Ni electrodes show better hydrogen evolution efficiency than the pure Ni electrode [18, 19]. It originates due to the modification of the surface of Pd-Ni electrode. The secrecy is that on alloying, electrode surface modification could be achieved. Actually, when the alloy components establish a solid solution, it rarely retains the crystallographic structure of its original single components. Pd and Ni metals establish a solid solution in all ranges of their compositions [20, 21]. In such a state, predomination of Pd over Ni or vice versa might be expected [20]. If so, surface modification actions of Pd-Ni electrode may offer better electrocatalytic activity for the oxygen evolution during electrolysis.

In this context, the present study attempted to find out the electrochemical surface reaction behaviors, oxygen evolution characteristics and efficiencies, surface reaction kinetics of a Pd80at.%Ni alloy electrode. In preparing the PdNi alloy, higher proportion of Ni metal than Pd metal is utilized to preserve the price of the electrode at a minimum

and keep the method economical. Alkaline electrolyte medium (30wt.%KOH) is chosen because of having corrosion resistance capability of Pd and Ni in this medium than that in the acidic medium [13, 14].

2. Materials and Methods

Palladium and nickel of purity 99.9 wt.% were procured from Tanaka Kikinjoku Kogyo, Japan, and then processed to form Pd80at.%Ni alloy by arc melting at the Department of Materials Science and Engineering, Nagasaki University, Japan. The achieved alloy was then annealed. To construct electrode, it was then rolled into a sheet of 1 mm thick, cut into square size, re-annealed, connected with a nickel wire of diameter 0.1 cm and insulated, the process being elaborated elsewhere [3]. The geometric surface area of the constructed electrode was 0.79 cm^2. A nickel sheet of area 9.25 cm^2 was chosen as the counter electrode. For taking away any oxides present on the surface of the electrodes, their surfaces were chemically etched, polished thoroughly with a slurry of 0.3 μm Al_2O_3 powder, degreased with acetone and washed with ultrapure water. 30wt.%KOH solution was chosen to use as the electrolyte and it was prepared from reagent grade KOH pellets. A standard three-electrode (working, counter and reference electrode) cylindrical cell system was used for the experimental investigations where the electrodes were immersed in 100 ml dissolved oxygen free 30wt.%KOH electrolyte. A laminar flow of nitrogen was maintained over the surface of the electrolyte for preserving an inert atmosphere. Cyclic voltammetric (CV) measurements were carried out by EG&G PARC Model 362 potentiostat/Galvanostat. Current-potential (I vs. V) responses were drawn by EG&G PARC Model RE 0089 X-Y recorder.

The electrode surface characteristics and its oxygen evolution behavior were investigated by cycling it in between the potential range of – 1.0 to + 0.65 V at potential sweep rates of 20, 50, 100 and 200 mV/s. Time dependent study was carried out in between the potential range of – 0.2 to + 0.65 V by using a single scan rate of 100 mV/s. To understand the effect of switching negative potential if any on the electrode surface reactions and oxygen evolution, investigation was done by varying negative potential from – 1.0 V to – 0.3 V. For the determination of the kinetic parameters, i.e., Tafel slope (*b*) and exchange current density at zero overpotential (i_0) of the OER, continuous potential sweep method was used starting from the potential range of – 0.2 to + 0.73 V. Potential sweeps were carried out by varying the anodic potential towards negative potential initially 0.01 V and then 0.02 V. The final potential rage was – 0.2 to + 0.50 V. The sweep rate was 100 mV/s. All the voltammetric measurements were carried out at 298 K.

3. Results and Discussion

Fig. 1 shows the peaks and the lattice planes of the prepared Pd80at%Ni alloy identified from its X-ray Diffraction (XRD) pattern. It can be seen that four clear peaks appeared in the XRD pattern which originated from (PdNi)111, (PdNi)200, (PdNi)220 and (PdNi)311 planes. The peaks are positioned at 2θ values of 43.7°, 50.9°, 74.7° and 90.8°, respectively. Absence of peak for any other

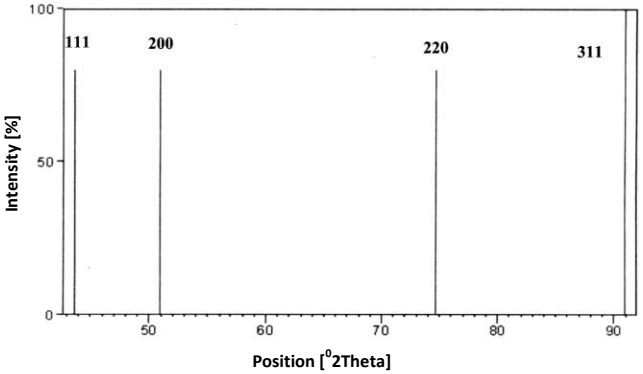

Fig. 1: Position of the XRD peaks and the planes identified for Pd 80 at.%Ni alloy

foreign element than that of Pd and Ni is indicating that the prepared alloy is free from impurity. The lattice parameter of the alloy is found to be 3.591Å which is smaller than that of Pd (3.891Å) but larger than that of Ni (3.524Å) precursor materials. It signifies that the prepared PdNi alloy is a lattice contracted alloy.

Fig. 2 represents the cyclic voltammograms appeared for the Pd80at.%Ni electrode in 30wt.%KOH electrolyte in between the potential range of – 1.0 V to + 0.65 V at 298 K at the scan rates of 20, 50, 100 and 200mV/s, respectively.

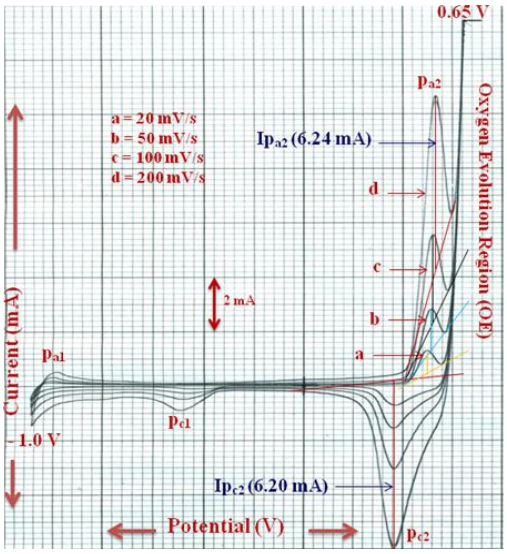

Fig. 2: Cyclic voltammograms appeared for the Pd80at.%Ni electrode in between the potential range of – 1.0 V to + 0.65 V in 30wt.%KOH electrolyte at different scan rates [20, 50, 100 and 200 mV/s] at 298 K

From Fig. 2, it is understand that the Pd80at%Ni electrode surface encountered a number of oxidation and reduction events. At least two different oxidation peaks designated as p_{a1} and p_{a2} and two reduction peaks designated as p_{c1} and p_{c2} appeared in the voltammograms. Current for the peaks

p_{a2} and p_{c2} remarkably increased with increasing the scan rates. The oxidation peak p_{a2} significantly moved to the positive potential direction and the differences in peak potentials between the p_{a2} and p_{c2} i.e, $\Delta E_{p22} = (E_{pa2} - E_{pc2})$, gradually increased with increasing the scan rate. The ΔE_{p22} value reached to 159 mV from 122 mV while increasing the scan rate from 20 to 200 mV/s. Such a large increase in potential differences between two peaks with scan rates is signifying that the electrochemical process possesses large irreversibility.

It was identified earlier that the peaks p_{a2} and p_{c2} are the redox couple of (PdNi)(II) ↔ (PdNi)(III) transformations [22]. The observed ΔE_{p22} values for these transformations are implying that in these steps the electron transfer process is very sluggish and the process irreversibility increased with increasing scan rate. Concentrating on the redox peak currents, it is observed that their ratio (Ip_{a2}/Ip_{c2}) stands to be almost unity. This behavior indicates that the (PdNi)(III) species generated on the electrode surface during oxidation completely reduced to the precursor oxide (PdNi)(II) during reduction. It is a sign of electrochemical process reversibility. But practically, the net redox process can be considered to be irreversible. To find out the reason of deviation of the net redox process from the reversibility, it was vital to check the peak current (Ip) vs. root of scan rate ($V^{1/2}s^{-1/2}$) behavior. This is a well accepted diagnosis to understand the cause of such anomaly. Fig. 3 shows the Ip_{a2} vs. $V^{1/2}$ plot.

It may be seen that Ip_{a2} and $V^{1/2}$ shows a linear relationship but the linearity is not continued up to the origin of the plot. Such a behavior implies that the redox process is not depending on the mass transport of OH^- ions of the electrolyte media. It seems realistic because the (PdNi)(II) species i.e. $(PdNi)(OH)_2$ forms first on the bare PdNi(0) electrode surface where the mass transport of OH^- ions is crucial. However, such a behavior of electrode surface seems to be a common factor in electrolysis process of Ni, Pd and PdNi electrodes of different compositions [3, 16, 22].

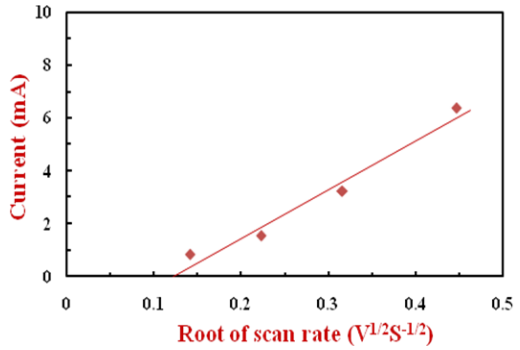

Fig. 3: Dependence of peak currents with the square root of scan rates of Pd80at.%Ni electrode in 30wt.%KOH electrolyte

It was vital to realize the origin of the formation of (PdNi)(III) species in the reduction pathway which reduces to (PdNi)(II) species through the peak P_{c2}. In fact, there are other electrochemical steps in the oxidation-reduction pathways through which gaseous oxygen evaluated from the species generated on the electrode surface. It is known that oxygen evolution reaction (OER) is such a demanding reaction step which composes of four electron transfers and O-O bond formation [6, 7]. It involves multiple electrochemical steps with at least one electron transfer per step. In the present case, in the oxidation pathway, up to the generation of (PdNi)(III) species on the bare PdNi(0) surface, three electron transfer within two steps might be marked. These are two electron transfer for the generation (PdNi)(II) species over bare (PdNi)(0) and one electron transfer for the generation of (PdNi)(III) species from (PdNi)(II) species. So, there remains a further electrochemical step in which the fourth electron transfer occurred. The acceptable possibility is that in the next step, (PdNi)(III) species transformed to (PdNi)(IV) species by losing an electron. Thus the consecutive species formed on the Pd80at%Ni electrode surface in the oxidation pathway can be represented as $(PdNi)(OH)_2$, $(PdNi)_2O_3$ and $(PdNi)_2O_4$, respectively. It is mentionable here that the transformation of $(PdNi)_2O_3 \rightarrow (PdNi)_2O_4$ occurred only at the set final positive potential of + 0.65 V. It starts to generate from the potential of + 0.51 V at scan rate 100 mV/s. The reduction pathway started from + 0.65 V towards to the negative potential direction. With decreasing potential from + 0.65 V, each electroactive $(PdNi)_2O_4$ species decomposed to and reduced to a $(PdNi)_2O_3$ species and generates a single O atom. Two single O atoms then on combination chronologically liberate gaseous oxygen in the whole way as indicated oxygen evolution region in Figure 2. This is the origin of the formation of (PdNi)(III) species and O_2 evolution in the reduction pathway. The (PdNi)(III) species then reduces to (PdNi)(II) species through the peak P_{c2}.

It is understandable that oxygen evolution occurred over the PdNi electrode surface by abiding the necessary and successive reaction steps and consequently by combining two oxygen atoms. Considering the rational reaction steps, it is possible to propose a mechanism of OER including all other reactions commenced over the Pd80at%Ni electrode surface during cycling in the potential range of – 1.0 V to + 0.65 V. These are as follows:

Oxidation step 1

$$PdNi(0) + 2OH^- \rightarrow (PdNi)(OH)_2 + 2e \quad (1)$$

Oxidation step 2

$$(PdNi)(OH)_2 \rightarrow (PdNi)_2O_3 + H_2O + e \quad (2)$$

Oxidation step 3

$$(PdNi)_2O_3 \rightarrow (PdNi)_2O_4 + e \quad (3)$$

Decomposition and reduction step

$$(PdNi)_2O_4 + e \rightarrow (PdNi)_2O_3 + 1/2O_2 \quad (4)$$

Combination step (Tafel step)

$$1/2O_2 + 1/2O_2 \rightarrow O_2 \quad (5)$$

Reduction step 1

$$(PdNi)_2O_3 + e \rightarrow (PdNi)(OH)_2 \quad (6)$$

Reduction step 2

$$(PdNi)(OH)_2 + 2e \rightarrow (PdNi)(0) \quad (7)$$

Looking on the above electrochemical reaction steps, it may be speculated that the oxidation step (ii) is the rate limiting or the decisive step for the oxygen evolution. Because as many $(PdNi)(OH)_2$ molecules are generated on the electrode surface, equal number of $(PdNi)_2O_3$ molecules and equal number of oxygen atoms are forming to combine and thereafter for evolving molecular oxygen. The present study observed that this crucial oxidation reaction step is sluggish. Generally, the complete generation of the precursor of such a sluggish reaction takes time to be equilibrated. To understand the fact and to achieve maximum precursor molecule on the electrode surface, a time dependent study on this oxidation reaction step was carried out. The chosen range of potential was – 0.2 to + 0.65 V and the scan rate was 100 mV/s. Fig. 4 shows the cyclic voltammograms of a part of the time dependent study.

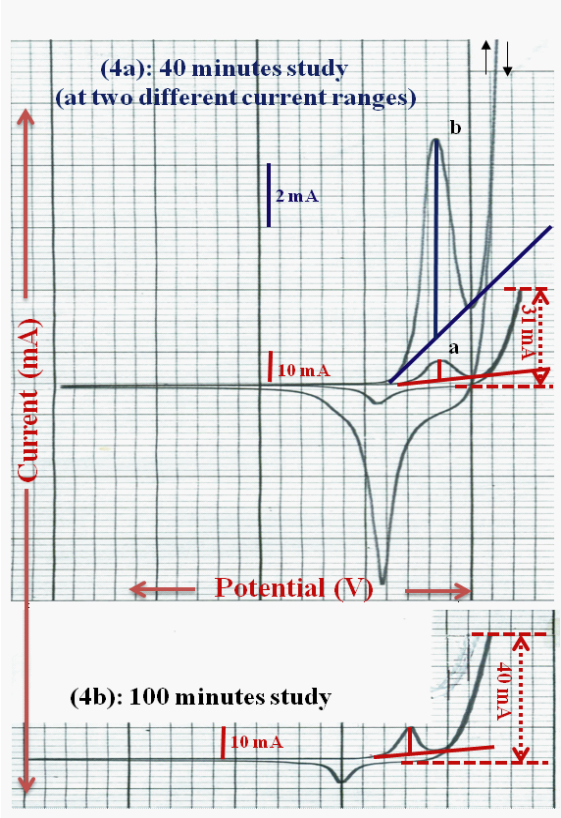

Fig. 4: Cyclic Voltammograms obtained for the Pd80at.%Ni electrode at (a) 40 minutes at two different current ranges and at (b) 100 minutes after cycling in between the potential range of – 0.2 V to + 0.65 V at the scan rate of 100 mV/s

From Figs. 4(a) - 4(b), it may be seen that the redox peak currents increased with increasing time. It may be seen that at the time of 40 minutes, the Ip_{a2} value is 6.2 mA (Fig. 4a). After 100 minutes, this value reached to 8.2 mA (Fig. 4b) whereas the initial Ip_{a2} value was only 3.3 mA (Fig. 2). It is notable that at time 100 minutes, almost saturation peak current was observed. Besides the enhancement of peak current with time other significant information is observed that with increasing peak current, the corresponding oxygen evolution current increased remarkably, i.e., oxygen evolution increased with time too. It may be seen that at 40 minutes, the oxygen evolution current is 31 mA (Fig. 4a) but it reached to a value 40 mA at and after 100 minutes (Fig. 4b). This finding also supports the assumption that the oxidation step: $(PdNi)(OH)_2 \rightarrow (PdNi)_2O_3$ is crucial for the OER over Pd80at.%Ni electrode surface.

Fig. 5 represents the cyclic voltammograms observed for Pd80at%Ni electrode at various potential ranges starting from initial potential – 1.0 V. The final potential was + 0.65 V. This study was carried out after activating the electrode at + 0.65 V for 100 minutes. It may be seen that

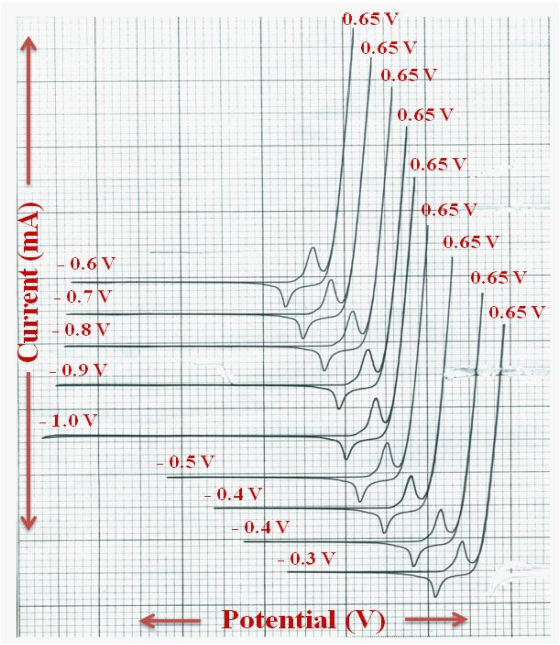

Fig. 5: Cyclic voltammograms of Pd80at.%Ni electrode in 30wt.%KOH electrolyte at various potential ranges at the scan rate of 100 mV/s

with the variation of starting negative potential from – 1.0 V to – 0.3 V, the redox peak currents for the transformations of $(PdNi)(OH)_2 \leftrightarrow (PdNi)_2O_3$ species and the corresponding oxygen evolution currents remained almost unchanged. It indicates that with the switching potential starting from – 1.0 V to – 0.3 V, the bare PdNi(0) electrode surface instantly covered by $PdNi(OH)_2$ as that observed by cycling in between – 0.2 to + 65 V up to 100 minutes as presented in Fig. 4(b). It informs that after proper activation of the electrode, the switching negative potential can be chosen to be – 0.2 V for the oxygen evolution studies of Pd80at%Ni electrode. However, further increase in switching potential to positive direction may affect the base line of the reduction peak p_{c2}.

In order to determine the kinetic parameters of the OER, oxygen evolution currents were recorded by drawing cyclic voltammograms at different potential ranges starting from

– 0.2 V to + 0.73 V. The experiment was carried out after activating the electrode at + 0.65 V for 100 minutes. Cyclic voltammograms were taken consecutively by decreasing the positive terminal potential towards negative potential direction at first in a step of 0.01 V (+ 0.73 V – 0.01 V = + 0.72 V) and then step of – 0.02 V (+ 0.72 V – 0.02 V = + 0.70 V and so on) at the scan rate of 100 mV/s. Various current ranges were applied in view to obtaining better response and better voltammograms. The observed cyclic voltammograms are shown in Fig. 6.

Fig. 6 shows that remarkable amounts of oxygen evolution occurred at all the investigated potential ranges. At the chosen final positive potential of + 0.73 V, the observed oxygen evolution current is 174.0 mA which is equivalent to the current density (*i*) of 220.25 mA/cm^2. It is notable that the surface area of the Pd80at.%Ni electrode is 0.79 cm^2. *i* value gradually decreased with decreasing the terminal positive potential value. At the potential values of + 0.70 V, + 0.60 V and + 0.50 V, the *i* values decreased to 176.71, 46.45 and 1.14 mA/cm^2, respectively.

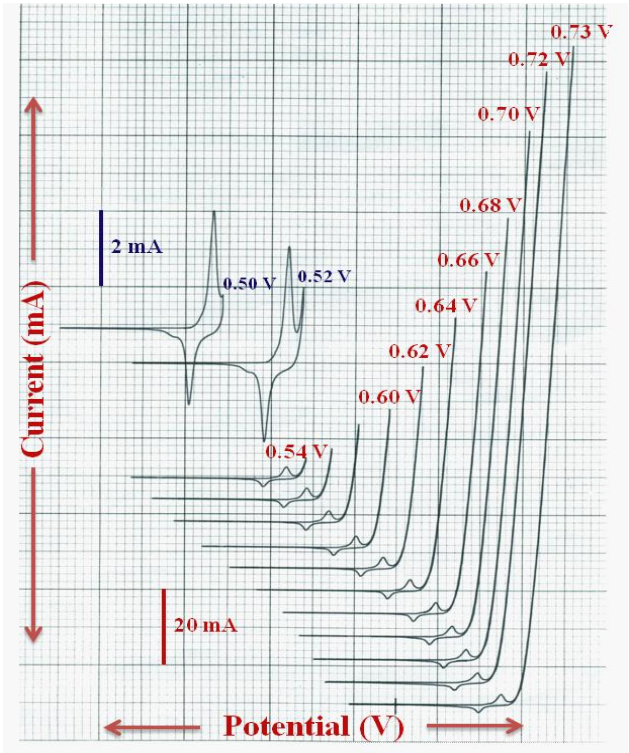

Fig. 6: Cyclic voltammograms obtained for the Pd-80at%Ni electrode at various potential ranges in 30wt.%KOH electrolyte at the sweep rate of 100 mV/s at 298 K

Fig. 7 shows the Tafel plot [Overpotential (η) vs. $\log_{Current\ density}$ (log*i*) plot] for the OER over the Pd80at.%Ni electrode. It was essential to draw this plot to find out the reaction kinetic parameters i.e., the exchange current density value at zero overpotential (i_o) and Tafel slope (*b*) value, and concurrently the efficiency of the electrode for the oxygen evolution through electrolysis. The η values are obtained by deducing the Hg/HgO.OH$^-$ reference electrode potential value + 0.30 V from the working potentials [3, 4]. It may be seen that the Tafel plot shows two well-defined Tafel regions as that observed for Ni electrode [3]. The region at low overpotentials is called low η region and the region at high overpotentials is known high η region. The obtained i_0 and *b* values for the low and high η regions are compiled in Table 1. It is notable that *b* values are calculated from the slopes of the Tafel lines and these are usually known as experimental values.

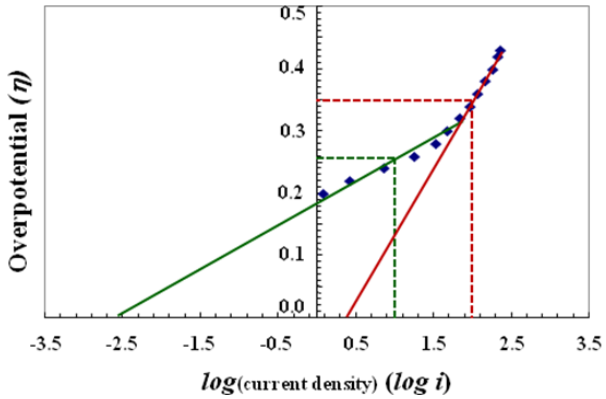

Fig. 7: Tafel plot for the oxygen evaluation reaction (OER) over the Pd80at.%Ni electrode in 30wt%KOH electrolyte at 298 K

Table 1: Tafel parameters for the oxygen evolution reactions (OER) over Pd80at.%Ni (present study) and Ni [3] electrodes in 30wt.%KOH electrolyte at 298 K

Electrode	Low η region				High η region			
	b (mV/dec)	i_0 (mA/cm^2)	η_{10} (mV)		b (mV/dec)	i_0 (mA/cm^2)	η_{100} (mV)	
			Calculated value	Practical value			Calculated value	Practical value
Pd80 at.%Ni			258.5	257.5	215.1	2.35	350.5	348.5
Ni [3]	82.0	2.82 x 10^{-3}	-	-	130.0	0.11	-	-

In view to justifying the obtained experimental values, it was crucial to check them by a different way. One of the ways is to calculate η value at a *i* value by putting the experimental values of i_o and *b* in the well known equation: $\eta_i = b \log_{10}(i/i_0)$ [3]. For the high η region, η value is calculated at the *i* value of 100 mA/cm^2 and for the low η region, η value is calculated at the *i* value of 10 mA/cm^2. The calculated values are also included in the Table 1. From the Table 1, it is clear that the calculated η values are almost equal to that of the experimental values. Such coincidence between the calculated and the experimental overpotential values is indicating that the experimental observations were well and good.

In view to understanding the difference in kinetic behaviors of Pd80at.%Ni electrode with those of a precursor material Ni electrode, its reported Tafel parameters, i_0 and *b* values for oxygen evolution are summarized in Table 1 too. It can be seen that for the low η region, presently observed i_0 value for Pd80at%Ni electrode is equal to that of Ni electrode and the *b* value is 9.2 mv/dec lower than that of it. On the other hand, for high η region, presently observed i_0 value is more than 21 folds higher and *b* value is about 85 mV/dec higher than those of Ni electrode. It indicates that addition of Pd with Ni significantly changed the kinetic values for the OER of Pd80at.%Ni electrode. It is

well established that in the field of electrolysis, the performance of an electrode mainly counts by considering the i_0 value. Higher i_0 value implies higher activity of the electrode for the OER [3, 17, 20]. In this sense, presently tested Pd80at.%Ni electrode can be considered to be an efficient electrode for the production of oxygen through electrolysis. In the high η region 21 folds higher i_0 value than that of Ni electrode is firmly indicating the development of a PdNi alloy electrode for the oxygen evolution in alkaline medium at room temperature is worth rewarding.

4. Conclusion

A Pd80at.%Ni electrode was constructed by arc melting of pure Pd and Ni, and then rolling, cutting, spot welding and packing with epoxy resin. The electrode surface characteristics, oxygen evolution behavior, surface reaction kinetics and electrode efficiency were investigated in a three electrode cell in 30wt.%KOH electrolyte at room temperature by utilizing cyclic voltammetry (CV). The CV diagrams of the electrode showed two oxidation and two reduction steps in between the potential range of – 1.0 to + 0.65 V. Sufficient number of CV diagrams were drawn up to 100 minutes in between the potential range of – 0.2 to + 0.65 V which enabled in obtaining the saturated layer of $(PdNi)_2O_3$ species over the Pd80at.%Ni electrode. CV diagrams were drawn by applying various potential ranges starting from – 0.20 V to 0.73 V in view to getting Tafel plot to find out the oxygen evolution reaction (OER) kinetics. From the Tafel plot, the kinetic parameters, i.e., the exchange current density at zero overpotential (i_0) and the slope (b) values were found out. A drive was given to justify the obtained experimental b values. A good coincidence was observed between the experimental and the calculated values. The observed kinetic parameters were judged with the available kinetic data of Ni electrode. Comparison of the data concluded that the presently constructed Pd80at.%Ni electrode gives better efficiency for the oxygen evolution through electrolysis in alkaline medium at room temperature.

Acknowledgement

One of the authors is very much grateful to Professor Y. Sakamoto, Department of Materials Science and Engineering, Nagasaki University, Japan, for giving permission to utilize Engineering Faculties Arc Melting Laboratory and facilitating annealing, processing and spot welding systems for constructing the Pd80at.%Ni electrode.

References

1. G. Kreysa and B. Haklansson, Electrolysis by Amorphous Metals of Hydrogen and Oxygen Evolution in Alkaline Solution, J. Electroanal. Chem., **201,** 61-83 (1986).
2. A. Mills, Heterogeneous Redox Catalysts for Oxygen and Chlorine Evolution, Chem. Soc. Rev., **18,** 285-316 (1989).
3. A. K. M. F. Kibria and M. Sh. Mridha, Electrochemical Studies of The Nickel Electrode For The Oxygen Evolution Reaction, Int. J. Hydrogen Energy, **21,** 179-182 (1996).
4. A. K. M. F. Kibria and S. A. Tarafrar, Electrochemical Studies of A Nickel-Copper Electrode For The Oxygen Evolution Reaction (OER), Int. J. Hydrogen Energy **27**, 879-884 (2002).
5. X. Li, F. C. Walsh and D. Pletcher, Nickel Based Electrocatalysts For Oxygen Evolution In High Current Density Alkaline Water Electrolysers, Phys. Chem. Chem. Phys.**, 13**, 1162-1167 (2011).
6. B. E. Conway, L. Bai and M. A. Sattar, Role of The Transfer Coefficient In Electrocatalysts: Applications to The H_2 and O_2 Evolution Reactions And The Characterization of Participating Adsorbed Intermediates, Int. J. Hydrogen Energy, **12**, 607-621 (1987).
7. M. T. M. Koper, Thermodynamic Theory of Multi-Electron Transfer Reactions: Implications For Electrocatalysis, J. Electroanal. Chem., **660,** 254-260 (2011).
8. V. I. Birss, A. Damjanovic and P. G. Hudson, Oxygen Evolution At Platinum-Electrodes In Alkaline Solutions: Mechanism of The Reaction, J. Electrochem. Soc., **133**, 1621-1625 (1986).
9. B. E. Conway and T. C. Liu, Characterization of Electrocatalysis In The Oxygen Evolution Reaction at Platinum by Evaluation of Behavior of Surface Intermediate States at The Oxide Film, Langmuir, **6,** 268-276 (1990).
10. C. C. L. McCrory, S. Jung, J. C. Peters and T. F. Jaramillo, Benchmarking Heterogeneous Electrocatalysts For The Oxygen Evolution Reaction, J. American Chem. Soc., **135,** 16977-16987 (2013).
11. S. Trasatti and H. Wendt (Ed.) The Oxygen Evolution Reaction in Electrochemical Hydrogen Technologies, Elsevier, Amsterdam, pp. 1-14 (1990).
12. D. E. Hall, Electrodes for Alkaline Water Electrolysis, J. Electrochem. Soc., **128**, 740-746 (1981).
13. F. M. Sapountzi, J. M. Gracia, C. J. Weststrate, H. O. A. Fredriksson and J. W. Niemantsverdriet, Electrocatalysts for the Generation of Hydrogen, Oxygen And Synthesis Gas, Prog. Energy and Combus. Sci., **58**, 1-35 (2017).
14. E. Fabbri, A. Habereder, K. Waltar, R. Kötz and T. J. Schmidt, Developments and Perspectives of Oxide-Based Catalysts For The Oxygen Evolution Reaction, Catal. Sci. Technol., **4**, 3800-3821 (2014).
15. I. J. Godwin and M. E. G. Lyons, Enhanced Oxygen Evolution At Hydrous Nickel Oxide Electrodes Via Electrochemical Ageing In Alkaline Solution, Electrochem. Commun., **32**, 39-42 (2013).
16. M. M. Jaksic, B. Johansen and R. Tunold, Electrochemical Behavior of Pd in Acidic and Alkaline Solutions of Heavy and Regular Water, Int. J. Hydrogen Energy, **18**, 111-124 (1993).
17. M. J. DE. Giz, J. C. P. DA. Silva, M. Ferreira, S. A. S. Machado, E. A. Ticianelli, L. A. Avaca and E. R. Gonzalez, Progress on the Development of Activated Cathodes For Water Electrolysis, Hydrogen Energy Progress, **VIII**, 405-414 (1990).
18. B. Pierozynski and T. Mikolajczyk, Application of Pd-Modified Nickel Foam Cathodes To The Process of Alkaline Water Electrolysis, Int. J. Electrochem. Sci., **11**, 4865-4877 (2016).

19. M. Sarker, M. A. I. Molla, R. Islam, S. Ahmed and A. K. M. F. Kibria, Investigations on the Redox Behavior and The Electrolysis Characteristics of Pd-20at.%Ni Electrode in 30wt.%KOH Electrolyte, Bangladesh J. Sci. and Indus. Res., **43**, 13-28 (2008).

20. J. M. Jaksic, N. V. Krstajic, B. N. Grgur and M. M. Jaksic, Hydridic and Electrocatalytic Properties of Hypo-Hyper-*D*-Electronic Combinations of Transition Metal Intermetallic Phases, Int. J. Hydrogen Energy, **23**, 667-681 (1998).

21. E. Wicke, H. Brodowsky and H. Zuchner, Hydrogen in Metals II, Springer, New York, 223 - 241 (1978).

22. R. Das, M. Shajahan, M. F. Alam and A. K. M. F. Kibria, Hydrogen Generation Characteristics and Efficiency of A Pd80at%Ni Electrocatalyst In Alkaline medium, J. Nucl. Sci. Appl., **24**, 45-50 (2015).